Full length article

Induction of mesenchymal stem cell chondrogenic differentiation and functional cartilage microtissue formation for *in vivo* cartilage regeneration by cartilage extracellular matrix-derived particles

Heyong Yin [a,b,1], Yu Wang [a,1], Zhen Sun [a], Xun Sun [a,b], Yichi Xu [a], Pan Li [a,c], Haoye Meng [a], Xiaoming Yu [a], Bo Xiao [a], Tian Fan [a], Yiguo Wang [a], Wenjing Xu [a], Aiyuan Wang [a], Quanyi Guo [a], Jiang Peng [a,*], Shibi Lu [a]

[a] Institute of Orthopedics, Chinese PLA General Hospital, 28th Fuxing Road, Beijing 100850, PR China
[b] School of Medicine, Nankai University, 94th Weijin Road, Nankai District, Tianjin 300071, PR China
[c] Hebei Medical University, 361th Zhongshan East Road, Shijiazhuang 050017, PR China

ABSTRACT

We propose a method of preparing a novel cell carrier derived from natural cartilage extracellular matrix (ECM), designated cartilage ECM-derived particles (CEDPs). Through a series of processes involving pulverization, sieving, and decellularization, fresh cartilage was made into CEDPs with a median diameter of 263 ± 48 μm. Under microgravity culture conditions in a rotary cell culture system (RCCS), bone marrow stromal cells (BMSCs) can proliferate rapidly on the surface of CEDPs with high viability. Histological evaluation and gene expression analysis indicated that BMSCs were differentiated into mature chondrocytes after 21 days of culture without the use of exogenous growth factors. Functional cartilage microtissue aggregates of BMSC-laden CEDPs formed as time in culture increased. Further, the microtissue aggregates were directly implanted into trochlear cartilage defects in a rat model (CEDP + MSC group). Gait analysis and histological results indicated that the CEDP + MSC group obtained better and more rapid joint function recovery and superior cartilage repair compared to the control groups, in which defects were treated with CEDPs alone or only fibrin glue, at both 6 and 12 weeks after surgery. In conclusion, the innovative cell carrier derived from cartilage ECM could promote chondrogenic differentiation of BMSCs, and the direct use of functional cartilage microtissue facilitated cartilage regeneration. This strategy for cell culture, stem cell differentiation and one-step surgery using cartilage microtissue for cartilage repair provides novel prospects for cartilage tissue engineering and may have further broad clinical applications.

Statement of Significance

We proposed a method to prepare a novel cell carrier derived from natural cartilage ECM, termed cartilage ECM-derived particles (CEDPs), which can support proliferation of MSCs and facilitate their chondrogenic differentiation. Further, the direct use of functional cartilage microtissue of MSC-laden CEDP aggregates for cartilage repair *in vivo* induced hyaline-like articular cartilage repair. This strategy for cell culture, stem cell differentiation and the one-step surgery for cartilage repair provide novel prospects for cartilage tissue engineering and may have further broad clinical applications.

© 2016 Acta Materialia Inc. Published by Elsevier Ltd. All rights reserved.

1. Introduction

Cartilage has a very limited capacity for self-repair and regeneration because of its avascular structure [1,2]. Researchers have been exploring effective treatment methods for cartilage injury and to prevent further deterioration of damaged cartilage [3]. Tissue engineering involving scaffold, cell sources, and growth factors serves as a promising alternative strategy for cartilage repair [4]. Nevertheless, several shortcomings still remained to be improved.

The cell source is one of the most important elements in cartilage tissue engineering. Clinically, chondrocytes as the best-reported cell sources are mainly obtained from biopsies of

non-weight-bearing areas of joints [5]. However, it is difficult to harvest sufficient cell numbers due to the low density of chondrocytes in cartilage, and biopsies of native cartilage may result in donor site morbidity [6]. Moreover, chondrocytes easily lose their chondrogenic phenotype with increasing passage number in two-dimensional plate culture, which resulting in the production of inferior extracellular matrix [7]. Therefore, alternative cell sources and culture methods have been investigated to overcome these shortcomings.

Mesenchymal stem cells (MSCs) are promising alternative cell sources for cartilage tissue engineering due to their ease of harvest, chondrogenic differentiation potential, and rapid proliferation abilities [8,9]. Extensive research using MSCs as the cell source has achieved satisfactory results for *in vivo* repair of articular cartilage defects [10–12]. Microcarrier culture technology for chondrocyte culture was first introduced by Freed [13], who reported that chondrocytes can be expanded on microcarriers with higher yield compared to static cultures [13]. Subsequent studies by multiple groups confirmed that microcarrier culture improved the maintenance of the chondrogenic phenotype and redifferentiation of articular chondrocytes [14–16]. In addition, microcarrier culture of MSCs promoted their proliferation and differentiation [17,18]. Bioreactor systems can provide a uniform and favorable environment for microcarrier culture. Many commercial microcarriers, including dextran, plastic, glass, gelatin are currently available [19]. To improve biocompatibility, some extracellular matrix components were introduced onto commercial microcarriers [20]. For example, Cytodex-3 with a thin layer of denatured pig skin-derived collagen on its surface to increase its biocompatibility, is more conducive to cell adhesion compared to Cytodex-1. The stem cell microenvironment is the key to cell differentiation along the appropriate lineage. The ECM is a specific mixture of substances secreted by resident cells, which not only provides a suitable place for cell growth activity, but also affects the differentiation of stem cells [21]. Many studies have reported that cartilage ECM components can promote chondrogenic differentiation of stem cells [21–24]. Researchers also used cartilage fragments or minced cartilage directly to promote cartilage repair [25–27]. We postulated that a microcarrier derived from cartilage ECM would not only have good biocompatibility, but may also promote chondrogenesis of stem cells by providing a natural cartilage-like environment.

Here, we propose a method for preparing a novel cell carrier derived from cartilage ECM, and further cartilage microtissue formation for cartilage repair. Fresh goat knee joint cartilage fragments were shattered into particles, and those with median diameter of 263 ± 48 μm were selected, as this approaches the size of commercial microcarriers and facilitates further decellularization. We found that bone marrow stromal cells (BMSCs) can be expanded on the surface of CEDPs with high viability, and differentiated into chondrocyte lineage after 21 days of culture in a rotary cell culture system (RCCS) bioreactor without the use of exogenous growth factors. With increasing time in culture, CEDPs became connected by matrix secreted from MSCs, forming cartilage microtissue aggregates. Further, the functional microtissue aggregates of cell-laden CEDPs were used directly for *in vivo* cartilage repair and led to native hyaline-like articular cartilage repair. This strategy avoids the cell injury and loss of ECM caused by trypsin digestion along with 2D cell passage cultivation. Moreover, it also provides a promising single-step surgery using cartilage microtissue for cartilage treatment, in which BMSCs are isolated from the patient before surgery, expanded on the CEDPs in a bioreactor for several days to form microtissue aggregates, and then directly reimplanted into the patient.

2. Materials and methods

2.1. Experimental design

An overview of the research design is shown in Fig. 1. Through a series of processes involving pulverization, sieving, and decellularization, fresh goat knee joint cartilage was made into particles with a median diameter of 263 ± 48 μm. Green fluorescence protein (GFP)-labeled BMSCs were co-cultured with cartilage ECM-derived particles (CEDPs) in a microgravity rotary cell culture system (RCCS; Synthecon, Houston, TX). Functional cartilage microtissue aggregates of GFP-labeled MSC-seeded CEDPs after 21 days of culture, or CEDPs without cells, were implanted into cartilage defects in the rat trochlear groove. Fibrin glue was used to secure the implants. Cartilage defects filled with only fibrin glue served as controls. Gait analysis, along with histological and mechanical evaluations and micro-CT analysis, were conducted at 6 and 12 weeks after surgery.

2.2. Preparation of cartilage ECM derived particles

2.2.1. Pulverization of goat knee articular cartilage

Fresh goat knees were obtained from a local slaughterhouse, and then articular cartilage was collected with a knife in a bioclean environment. After suspension in sterile phosphate-buffered saline (PBS), pH 7.6, cartilage pieces were pulverized physically into tiny particles with a tissue pulverizer (DJ13B-C669SG; Jiuyang, Jinan, China). To ensure that cartilage particles were of an appropriate size, they were suspended in PBS were filtered through a steel sieve with 300-μm pores (VWR® Testing Sieves; VWR, Radnor, PA). The siftings were then passed through another sieve with 150-μm pores. After these steps, cartilage ECM-derived particles with approximately 150–300 μm in diameter were harvested, and suspended in PBS for subsequent processes.

2.2.2. Decellularization of cartilage ECM-derived particles

Cartilage-ECM derived particles were decellularized by incubation with different detergents at various concentrations, specifically 0.5%, 1%, and 2% sodium dodecyl sulfonate (SDS), or 1% and 3% Triton X-100, to determine a satisfactory method for decellularization. All reagents were purchased from Sigma–Aldrich (Poole, UK), unless otherwise specified. For each detergent treatment group, aliquots of 1 g of CEDPs (wet weigh) were immersed in 5 mL of chemical extraction solution in a thermostatic oscillator (XT-FL079; Thermo, Waltham, MA) for 8 h at 4 °C, followed by a further 4 h of treatment with 5 mL of deoxyribonuclease I (50 U/mL) and ribonuclease A (1 U/mL) at 37 °C. CEDPs were rinsed 10 times with PBS to remove excess chemical reagents. After sterilization by ^{60}Co γ irradiation, CEDPs were stored at 4 °C for further use.

2.3. Characterization of the cartilage ECM-derived particles

2.3.1. Morphological observation of decellularized CEDPs

After fixation in 10% neutral buffered formalin, CEDPs were examined under a stereoscope (Zoom.v16; Zeiss, Oberkochen, Germany). For scanning electron microscopy (SEM) (S-520; Hitachi, Tokyo, Japan), samples were fixed in 10% neutral buffered formalin, dehydrated in a graded ethanol series, subjected to critical point drying, and sputtered with gold. The particle size distribution was determined using a laser particle size analyzer (BT 9300Z; Malvern Instruments, Shanghai, China).
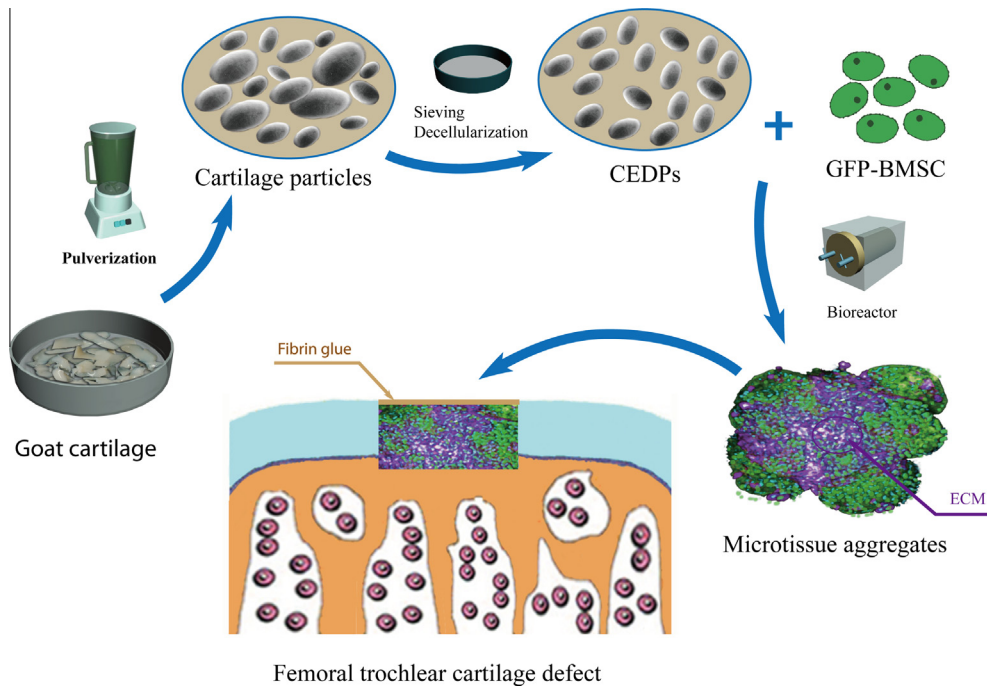
Fig. 1. Schematic illustration of the overall research design.

2.3.2. Histological and immunohistochemical evaluation

The CEDPs were fixed for 30 min in 10% neutral buffered formalin at room temperature, embedded in paraffin, and cut into sections 7 μm thick. Toluidine blue and safranin O staining was performed to detect GAG contents. To determine the composites of CEDPs, immunoflourescence for collagen I, collagen II, and aggrecan was conducted. For collagen I, epitope unmasking was carried out by hyaluronidase treatment for 15 min. For collagen II and aggrecan, epitope unmasking was carried out by Proteinase K (2.0 m g/mL) treatment for 1 h at 37 °C. The sections were then stained with primary antibodies (all from Abcam) to collagen I (1:500; Cat# ab3773), collagen II (1:100; Cat# ab34712), and aggrecan (1:500; Cat# ab140707) at 4 °C overnight. After 60 min incubation of secondary antibodies, 5 min counterstain of nuclei with Hoechst 33258 (Molecular Probes, Eugene, OR), images were taken from an Olympus fluorescence microscope.

2.3.3. Sulfated GAG, hydroxyproline and DNA quantification

Samples were digested with papain cocktail (125 mg/mL papain, 5 mM EDTA, 5 mM L-cysteine, and 100 mM phosphate buffer, pH 6.5) at 60 °C overnight. Subsequently, the total sGAG content was determined by 1,9-dimethylmethylene blue dye (DMMB) assay. The total hydroxyproline content was detected with a hydroxyproline detection kit (Sigma, Poole, UK). The DNA content was quantified using a PicoGreen DNA kit (Invitrogen, Carlsbad, CA) according to the manufacturer's protocol.

2.4. In vitro studies of cell expansion on CEDPs

2.4.1. Generation of GFP-labeled BMSCs

With ethical approval from the Institutional Animal Care and Use Committee of Chinese PLA General Hospital, bone marrow stromal cells were isolated from bone marrow aspirates from six male Sprague–Dawley rats (300–350 g) and cultured as described previously by Maniatopoulos [28]. Briefly, cell suspensions were plated in α-MEM supplemented with 10% FBS, 100 U/mL penicillin, and 100 μg/mL streptomycin. At passage 1, BMSCs were infected with GFP lentivirus (LVPEG; Cyagen, Santa Clara, CA) for labeling with green fluorescent protein. MSCs from the third passage were used.

2.4.2. Cell seeding on CEDPs and induction of differentiation in vitro

For cell seeding, BMSCs and CEDPs were co-cultured in a rotary cell culture system (RCCS; Synthecon) (condition MSC + CEDP + MG). Specifically, aliquots of 100 mg of CEDPs (wet weight) were rinsed three times with sterile PBS, pre-cultured with DMEM-low glucose (DMEM-LG) supplemented with 10% fetal bovine serum, penicillin 100 U/mL, streptomycin 100 mg/mL, and 2 mM L-glutamine overnight, and then transferred into an RCCS vessel with 50 mL of cell suspension containing 2×10^6 rat BMSCs in DMEM-LG supplemented with 10% FBS. To facilitate the adhesion of BMSCs to CEDPs, rotation was set as 20 rpm for 1 min with a 30-min pause for the first 24 h, and then cells were cultured with continuous rotation at 50 rpm. The RCCS was placed in a 37 °C 5% CO_2 incubator. Static cultures of MSCs with CEDPs were also performed as control (condition MSC + CEDP + ST). When MSCs were cultured alone, the medium was supplemented with 10 ng/mL TGF-β3 (condition MSC + TGF-β3). The culture medium was changed every 2–3 days. After 21 days in culture, microtissue aggregations of GFP-BMSCs laden CEDPs were prepared for *in vivo* implantation.

2.4.3. Cell viability and proliferation assessment

Cell viability and proliferation of BMSCs cultured on CEDPs after 1, 7, 14 and 21 days were demonstrated by Live/Dead Cell Viability Assay (Life Technologies, Carlsbad, CA) and DNA quantification. Briefly, aggregations of BMSCs and CEDPs were rinsed with PBS and stained for 5 min at room temperature in 5 μg/mL fluorescein diacetate (FDA) and 5 μg/mL propidium iodide (PI) [10]. Images were examined by fluorescence microscopy. For Live/Dead staining, BMSCs were not transfected with GFP. The DNA content was quantified using a PicoGreen DNA kit (Invitrogen, Carlsbad, CA) according to the manufacturer's protocol.

2.4.4. RNA isolation and quantitative polymerase chain reaction (qPCR)

After 21 days of co-culture with CEDPs, total RNA was isolated from cells using TRIzol reagent (Invitrogen) according to the manufacturer's protocol. Reverse transcription was conducted using an

iScript cDNA Synthesis kit (Bio-Rad, Richmond, CA), and then qPCR was performed with denaturation at 95 °C for 5 min followed by 40 cycles of 95 °C for 15 s, 60 °C for 15 s and 72 °C for 15 s. The $\Delta\Delta Ct$ method was used to analyze the qPCR results. The primers designed for qPCR are as follows: Col1A1 (forward 5′- GATGGCCT GAAGCTCAA-3′ and reverse 5′-GGT TTGTTGAAGAGGCTG-3'), Col2A1 (forward 5′-GCACCCATGGACATTGGAGGG-3′ and reverse 5′- GACACGGAGTAGCACCATCG-3′), SOX-9 (forward 5′-CGTGGTGA CAAGGGTGAGAC-3′ and reverse 5′-TAGGTGATGTTCTGGGA GGC-3′), Aggrecan (forward 5′-TTCATGAAGATGACCGACGA-3′ and reverse 5′-CACACCATGAAGGCGTTCAT-3′), COL10A1 (forward 5′-G CAACTAAGGGCCTCAATGG-3′ and reverse 5′-CTCAGGCATGACTGCT TGAC-3′), COMP (forward 5′-CCGACAGCAACGTGGTCTT-3′ and reverse 5′-CAGGT TGGCCCAGATGATG-3′), GAPDH (forward 5′-CC ACTTTGTGAAGCTCATTTCCT-3′ and reverse 5′-TCGTCCTCCTCTGGT GCTCT-3′).

2.5. In vivo experiment

2.5.1. Rat femoral trochlear cartilage defect model and repair with GFP-BMSC-loaded CEDPs

Seventy-two healthy male Sprague–Dawley rats weighing 300–350 g were used according to protocols approved by the Institutional Animal Care and Use Committee at Chinese PLA General Hospital. Animals were anesthetized with 3% sodium pentobarbital (40 mg/kg body weight, i.p.), and then an osteochondral defect (2 mm in diameter and 2 mm in depth) was created with a sterile biopsy punch in the center of the trochlear groove of the right leg. Rats were randomly divided into three groups according to the implant: the CEDP + BMSC group, in which prepared microtissue aggregates of GFP-BMSC laden CEDPs were implanted into the cartilage defects, and fibrin glue was applied to the surface to secure the grafts; the CEDP group, in which CEDPs were implanted alone into the defects, and Fibrin glue was used to maintain the CEDPs; and the fibrin group, in which cartilage defects were filled with fibrin glue alone. The rats were sacrificed by CO_2 asphyxiation at 6 or 12 weeks after surgery.

2.5.2. Catwalk for gait analysis

Gait analysis was conducted on walking rats ($n = 6$) at 1, 3, 6, and 12 weeks after surgery using the catwalk method (CatWalk XT; Noldus, Wageningen, The Netherlands) [29]. The mean intensity (arbitrary units, a.u.), which reflects the pressure exerted by the paw and paw area (cm^2) representing the floor area contacted by the paw during stance phase, were measured to evaluate joint function of the experimental right leg.

2.5.3. Fluorescence imaging and gross morphological evaluation

Knee joints were examined immediately using Kodak In-Vivo Imaging Systems FX (Kodak, Tokyo, Japan) to track the GFP-BMSCs in the repaired area at 2 and 12 weeks after surgery, as described previously [10]. Gross morphological evaluation were then performed for each knee to evaluate defect filling, surface smoothness, and tissue integration [30].

2.5.4. Histological and immunohistochemical evaluation

Samples ($n = 4$) were fixed for 2 days in 4% paraformaldehyde, decalcified in 10% (w/v) EDTA for 3–4 weeks, embedded in paraffin, and cut into sections 7 μm thick. Hematoxylin and eosin (H&E) staining was performed for morphological evaluation, and toluidine blue staining was performed for glycosaminoglycan content analysis. For detection of GFP-labeled cells in the repaired area, samples ($n = 4$) were also embedded in OCT for cryosectioning. Immunohistochemistry was conducted using primary antibodies (all from Abcam) to collagen I (1:500; Cat# ab6380) and collagen II (1:100; Cat# ab34712). For collagen II, epitope unmasking was

carried out by Proteinase K (2.0 m g/mL) treatment for 1 h at 37 °C. For collagen I, epitope unmasking was carried out by hyaluronidase treatment for 15 min. For histological scoring of repaired tissues within the defect, the histological sections from the lateral and medial regions of each defect (total, 30 images per group) were blindly scored by three independent evaluators based on the Wakitani scoring system [31].

2.5.5. Mechanical analysis

Indentation test was performed to evaluate the mechanical properties of the repaired tissue ($n = 4$) at 12 weeks using a mechanical test machine (ElectroForce 3320; Bose, Eden Prairie, MN) according to reported methods [32]. A five-step continuous displacement control method was used to obtain the balancing load value, and the thickness of the cartilage was measured by the probe method. Young's modulus was then calculated using the following formula: $E = P (1 - v^2)/2auk$ (P, elastic modulus; v, Poisson's ratio; a, indenter radius; u, indenter displacement; k, theoretical adjustment coefficient).

2.5.6. Micro-CT analysis

Microcomputed tomography (micro-CT, GE, USA) was conducted to evaluate the bone regeneration level. Rabbit femur end simples ($n = 6$) were fixed for 2 days in 4% paraformaldehyde, and then placed in a sample holder for micro-CT scanning. To analyze the volume of bone in the defect, a cylindrical region of interest (ROI) 2 mm in diameter and 2 mm in thickness was selected.

2.6. Statistical analysis

Date are expressed as means ± standard deviation. After testing for homogeneity of variances, one-way analysis of variance (ANOVA) followed by Tukey's *post hoc* multiple comparisons test was used to determine the significance of differences between groups. SPSS 11.0 (SPSS, Chicago, IL) was used for statistical analyses, and $p < 0.05$ was taken to indicate statistical significance.

3. Results

3.1. Characterization of cartilage ECM-derived particles

Hoechst 33258, used to visualize DNA, revealed the presence of cells in CEDPs before decellularization. In contrast, almost no cell remnants were seen in CEDPs after decellularization with 1% SDS. Immunostaining for collagen I, collagen II, and aggrecan revealed that the CEDPs were positive for collagen II and aggrecan, but negative for collagen I before and after decellularization (Fig. 2).

The decellularization and preservation of the ECM of CEDPs were evaluated by quantitative analysis of DNA, GAG, and hydroxyproline contents. Among the five methods for decellularization, 1% SDS was chosen as the preferable decellularization protocol as it removed DNA to a great extent (97.24% DNA removal), which is essential for removal of the immunogenicity and retention of relatively high GAG components (88. 74% GAG). For hydroxyproline content, there was no significant difference between the five decellularization groups after the decellularization process (Fig. 3B–D).

After pulverization, sieving, and decellularization, the cartilage fragments were fabricated into particles, which were round, oval, or irregular in shape, as determined under a stereomicroscope (Fig. 3A1 and A2) and by scanning electron microscopy (Fig. 3A3). The higher magnification view of Fig. 3A3 shows that the edges of CEDPs comprise an interconnected network of collagen fibrils (Fig. 3A4). Toluidine blue staining (Fig. 3A5) and safranin O staining (Fig. 3A6), confirmed that the CEDPs were glycosaminoglycans (GAGs). The particle size distribution had a median
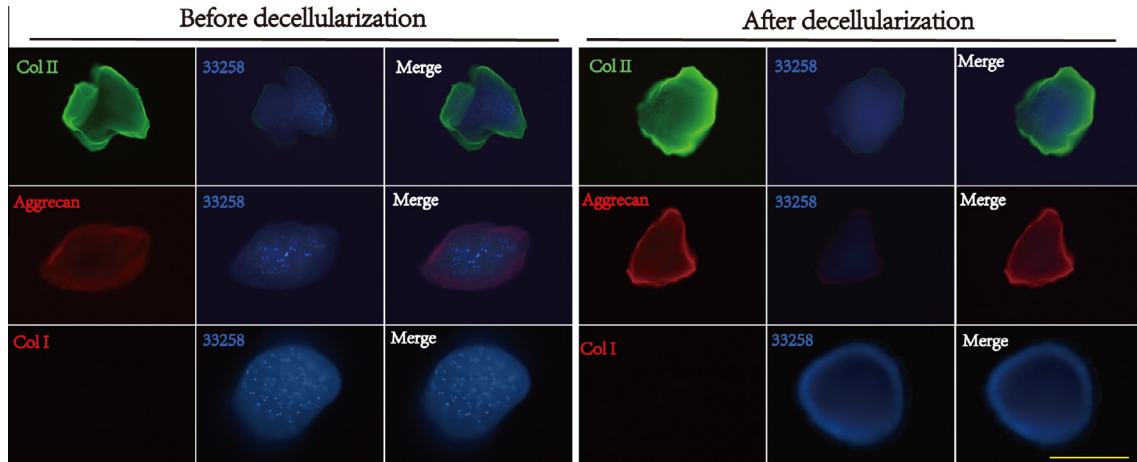
Fig. 2. Immunofluorescence staining of CEDP. Collagen I, collagen II, and aggrecan immunofluorescence staining of CEDP before and after decellularization.
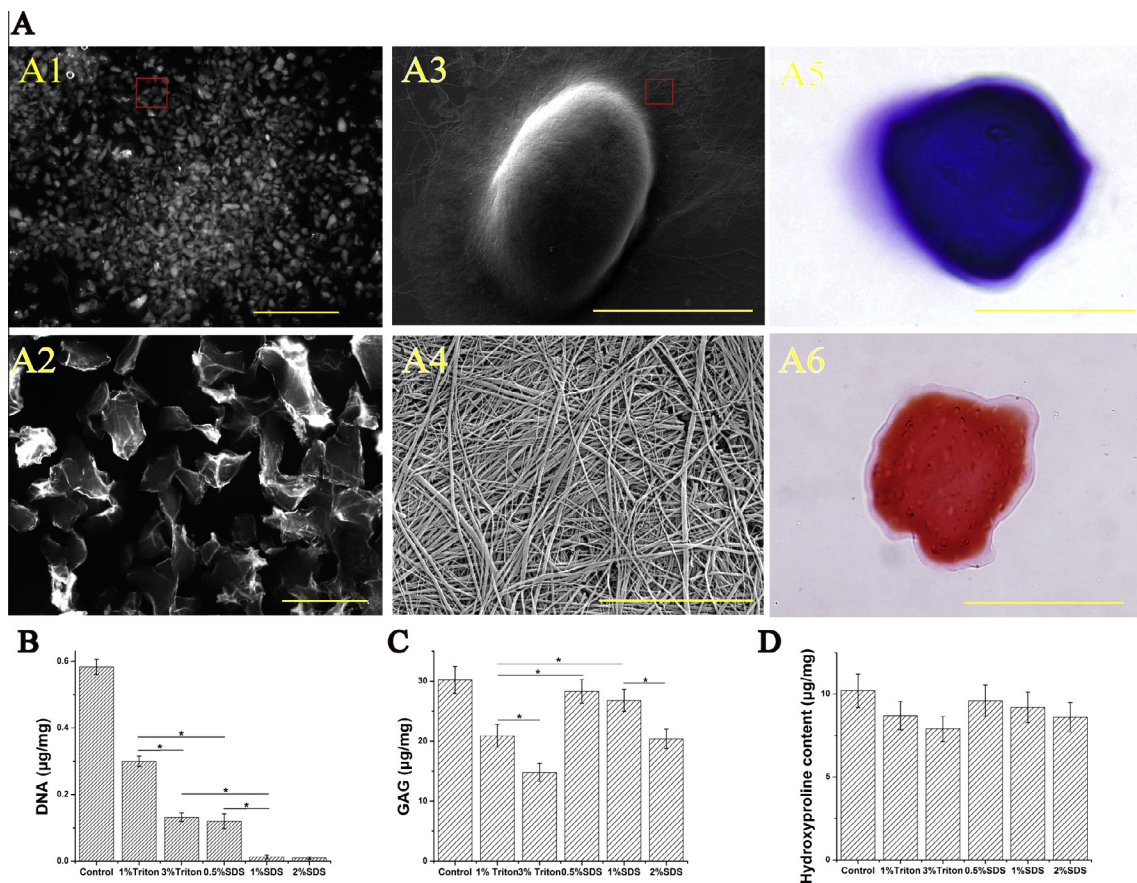

Fig. 3. Fabrication and characterization of CEDP. Stereoscopic images (A1, A2), scanning electron microscopy images (A3, A4), toluidine blue staining (A5), and safranin O staining (A6) of prepared CEDPs. The DNA content (B), GAG content (C), and hydroxyproline amount (D) in CEDP after decellularization. The red rectangle indicates the area shown on the right images at higher magnification. The results are the means ± SD (n = 5), $^*p < 0.01$. Scale bars: 200 μm in (A) and (A3, A5, A6), 2 mm in (A1), 500 μm in (A2), and 5 μm in (A4). (For interpretation of the references to color in this figure legend, the reader is referred to the web version of this article.)

diameter of 263 ± 48 μm, as determined using a laser particle size analyzer (Fig. 4).

3.2. Cell viability and proliferation

Cell proliferation on CEDPs and viability under microgravity were demonstrated by Live/Dead staining, scanning electron microscopy, and DNA quantification. As shown in Fig. 5A, MSCs can attach to CEDPs and proliferate rapidly on its surface with high viability over time. On day 1 post-seeding, viable cells (green fluorescence) were observed on the surface of CEDPs, while several dead cells (red fluorescence) were also seen (Fig. 5A). After 7 days of culture, viable cells with round morphology were expanded on the surface of CEDPs, and dead cells were found only occasionally. Cell-laden CEDPs were shown to aggregate into small clusters after 1 day in culture, and tended to become larger over time, forming
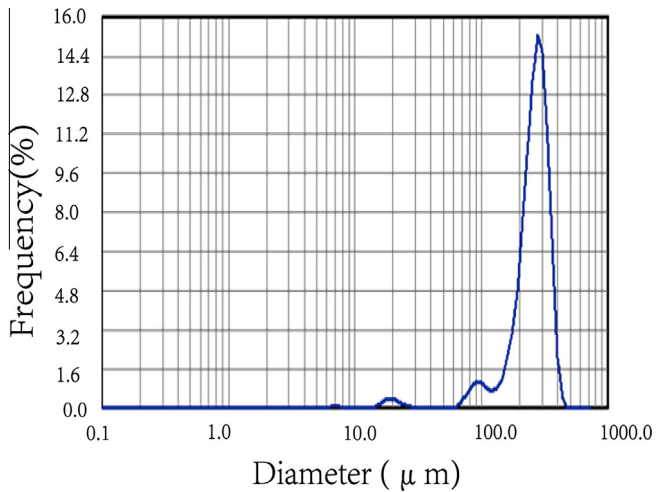
Fig. 4. The size distribution of CEDPs.

by matrix, whereas it was difficult to distinguish individual cells on CEDPs (Fig. 5B3 and B4). The DNA content of both MSC + CEDP + ST group and MSC + CEDP + MG group significantly increased during *in vitro* culture. At all the time point, the DNA content of MSC + CEDP + MG group was higher than that of MSC + CEDP + ST group (Fig. 6).

3.3. Chondrogenic differentiation in vitro

After 21 days of culture, toluidine blue (Fig. 7A–C) and immunohistochemical staining (Fig. 7D–F) were conducted to evaluate the deposition of proteoglycan and the expression of type II collagen. MSC + TGF-β3 served as a positive control group, which was positive for both toluidine blue staining and collagen II staining (Fig. 7C and F). This indicated that MSCs differentiated into mature chondrocytes after 21 days of culture in the presence of TGF-β3. When MSCs were co-cultured with CEDPs in a microgravity environment without exogenous TGF-β3 (MSC + CEDP + MG), cells were also found to be stained with toluidine blue, indicating the presence of proteoglycan (Fig. 7B). Strong staining for type II collagen was detected in central regions containing many chondrocyte-like cells (Fig. 7E). In the MSC + CEDP + ST group, toluidine blue staining was less intense than in the MSC + CEDP + MG group, and type II collagen staining was found only at discrete sites.

RT-qPCR was performed to determine the mRNA expression of several chondrogenic markers (ACAN, Col2A1, COMP, SOX9) after
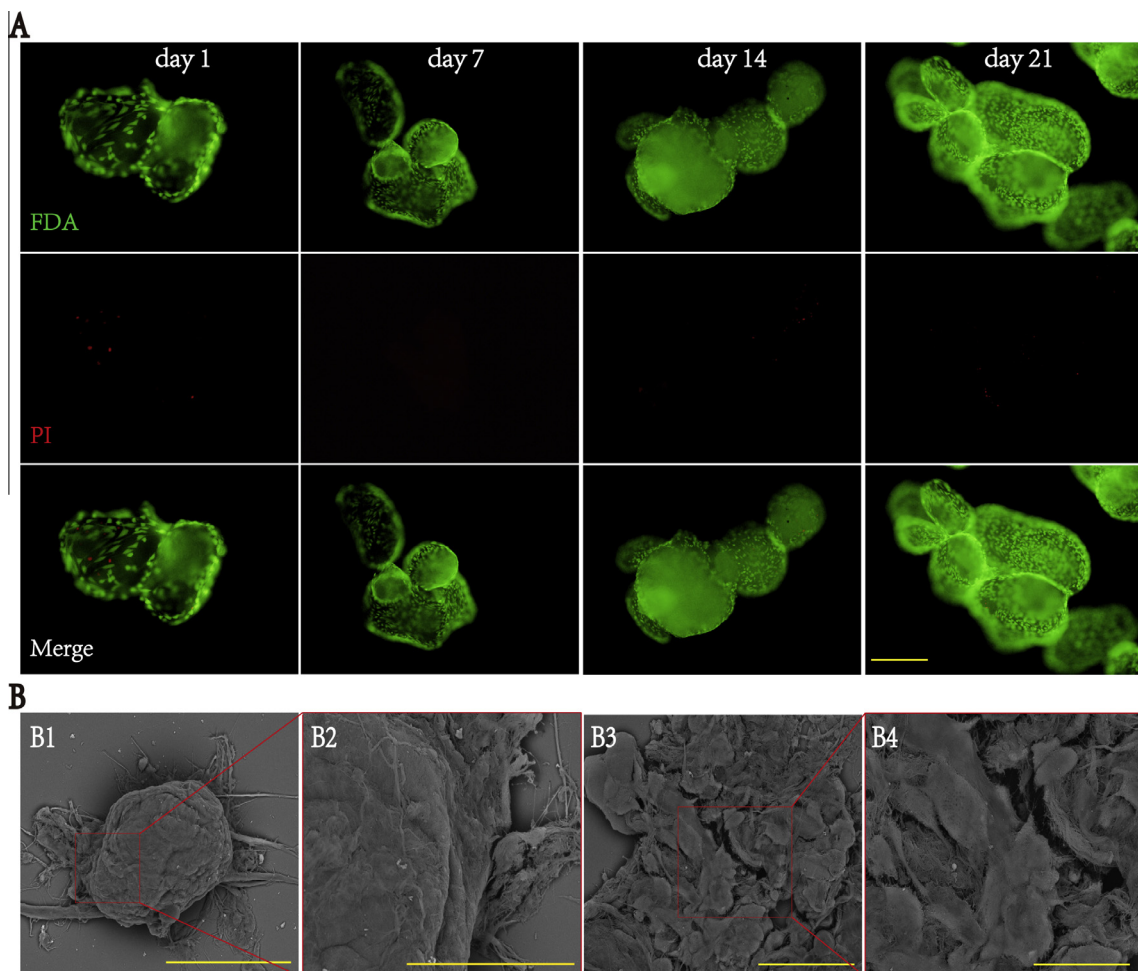
cartilage microtissue (Fig. 5A). Scanning electron microscopy showed that BMSCs attached and secreted matrix onto the surface of the CEDPs after 1 day of culture (Fig. 5B1 and B2). BMSC-laden microtissue aggregates at 21 days post-seeding were visualized by scanning electron microscopy, CEDPs were visibly connected

Fig. 5. The attachment and viability of BMSC on CEDPs. (A) Live (green fluorescence) and dead (red fluorescence) staining of BMSC-laden CEDP aggregates on day 1, day 7, day 14, and day 21 post-seeding. Scanning electron microscopy of CEDP laden with BMSCs at 1 day post-seeding (B1, B2), and microtissue aggregates after 21 days of culture (B3, B4). The red rectangle indicates the area shown in the right images at higher magnification. Scale bars: 200 μm in (A, B1), 100 μm in (B2), 50 μm in (B3), and 20 μm in (B4). (For interpretation of the references to color in this figure legend, the reader is referred to the web version of this article.)
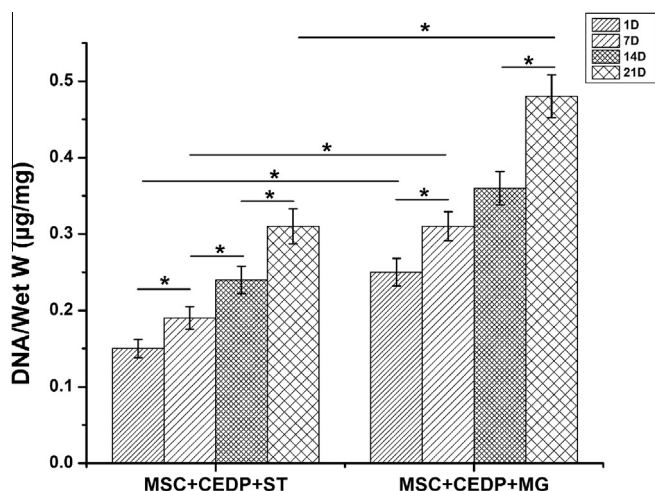
Fig. 6. The proliferation curve of MSC on CEDPs demonstrated by DNA quantification. MG indicates microgravity; ST indicates static.

21 days in culture (Fig. 7G, H, J, K). ACAN, Col2A1, and COMP expression were upregulated in the MSC + CEDP + ST group and MSC + CEDP + MG group compared to MSC on day 0, indicating differentiation into mature chondrocytes (Fig. 7G, H, J), and the MSC + CEDP + ST group showed significantly lower expression levels than the MSC + CEDP + MG group (p < 0.01). SOX9 expression, was upregulated in both the MSC + CEDP + ST group and MSC + CEDP + MG group compared to MSC on day 0, but the difference between the two groups was not statistically significant (p > 0.05) (Fig. 7K). Expression levels of the chondrogenic markers in the MSC + TGF-β group, which was used as a positive control group, were also upregulated compared to MSC on day 0 (p < 0.01) (Fig. 7G, H, J, K). The levels of COL1A1 expression in the MSC + CEDP + ST group, MSC + CEDP + MG group, and MSC + TGF-β group were significantly increased compared with MSC on day 0 (p < 0.01), while the expression level in the MSC + CEDP + MG group was lower than those in the two other groups (p < 0.01) (Fig. 7I). COL10A1, which is regarded as markers of hypertrophy, was also induced in the MSC + CEDP + ST group and MSC + CEDP + MG group at a similar level to that in the MSC + TGF-β group (Fig. 7L).

3.4. Gait analysis

Gait analysis was conducted using the catwalk method before and at 1, 3, 6, and 12 weeks after the operation to assess the experimental right knee joint function. Analysis of 3D footprint intensities of the right hind leg showed that the CEDP + MSC group had better footprint intensity recovery than the other two groups (Fig. 8A). As illustrated in Fig. 8B, the surgery and cartilage defects provoked a decrease in right hind leg intensity at 1 week after surgery in all groups, followed by a rising trend over time. The mean intensity of the CEDP + MSC group was higher than those of the two other groups at 3, 6, and 12 weeks after surgery (p < 0.01), indicating better recovery of joint function in this group. The paw area in the CEDP + MSC group was greater than those in the two other groups at 3, 6, and 12 weeks after surgery (p < 0.01) (Fig. 8C).

3.5. Macroscopic observation and histological evaluation

At 6 weeks after surgery, macroscopic observations showed that cartilage defects of the CEDP + MSC group were completely filled with white cartilage-like tissue with a flat surface and no obvious boundary between the neotissue and the surrounding

normal cartilage (Fig. 9A3). In contrast, the defects in the CEDP group and Fibrin group were partly filled with repair tissue with an irregular surface and distinct borders (Fig. 9A1 and A2). In the CEDP group and Fibrin group, the repair tissue was mostly fibrous tissue containing many spindle-shaped fibroblasts, while that in the CEDP + MSC group was mainly filled with hyaline-like cartilage as shown by H&E staining as well as toluidine blue staining (Fig. 9A4–A6, A10–A12). The neotissue in the CEDP group and Fibrin group showed little staining with toluidine blue (Fig. 9A10, A11, A13, A14), indicating poor GAG deposition. However, in the CEDP + MSC group, the repair tissue showed uniform toluidine blue staining, which was similar to the surrounding native cartilage (Fig. 9A12 and A15). The histological score of the CEDP + MSC group was higher than those of the other two groups (p < 0.01), and the CEDP group had a higher score than the Fibrin group (Fig. 10B) (p < 0.01).

At 12 weeks after surgery, macroscopic observation showed that the defects were almost filled completely with repair tissue in the three groups. However, the CEDP + MSC group had a smoother surface and better integration with the surrounding normal cartilage than the other two groups. The defects in the Fibrin group were still repaired with fibrous tissue, and those in the CEDP group were filled with a mixture of fibrous tissue and cartilage-like tissue. The CEDP + MSC group was repaired with hyaline-like cartilage, which was similar to normal cartilage (Fig. 9B4–B6, B10–B12). The neotissue in the Fibrin group was not stained with toluidine blue (Fig. 9B10 and B13), while lighter toluidine blue staining was observed in the CEDP group (Fig. 9B11 and B14). The repair tissue in the CEDP + MSC group showed intense toluidine blue staining, which was comparable to that of the surrounding normal cartilage, indicating superior cartilage repair (Fig. 9B12 and B15). The histological score of the CEDP + MSC group was higher than those of the other two groups (p < 0.01), and the CEDP group had a higher score than the Fibrin group (Fig. 10B) (p < 0.01).

### 3.6. Immunohistochemical analysis and Sirius red staining

In the CEDP + MSC group, the repair tissue was strongly positive for type II collagen antigen, while negative for type I collagen antigen at 6 and 12 weeks after surgery, which was similar to normal cartilage. In contrast, no areas positive for type II collagen were found in the Fibrin group, while type I collagen staining in this group was intense at either 6 or 12 weeks. In the CEDP group, the repair tissue was negative for type II collagen at 6 weeks, but weakly positive areas were seen at 12 weeks after surgery (Fig. 10A). Sirius red staining showed that the repaired tissue in the CEDP + MSC group was rich in type II collagen, and the collagen organization pattern was similar to that of surrounding native cartilage, while the repaired tissue in the CEDP and Fibrin groups was mostly type I collagen with irregular organization, as compared to surrounding normal cartilage (Fig. 11).

3.7. Biomechanical test

Young's modulus was examined at 12 weeks after surgery to assess the mechanical properties of the repaired tissue. Similar to normal cartilage, the repair tissue in the CEDP + MSC group had a significantly higher compressive modulus than the CEDP group or Fibrin group (p < 0.01). Moreover, the compressive modulus of the repair tissue in CEDP group was higher than that in the Fibrin group (Fig. 10C) (p < 0.01).

3.8. GFP-BMSC tracking

Furthermore, we investigated whether the implanted GFP-BMSCs remained in the defect sites and participated in cartilage
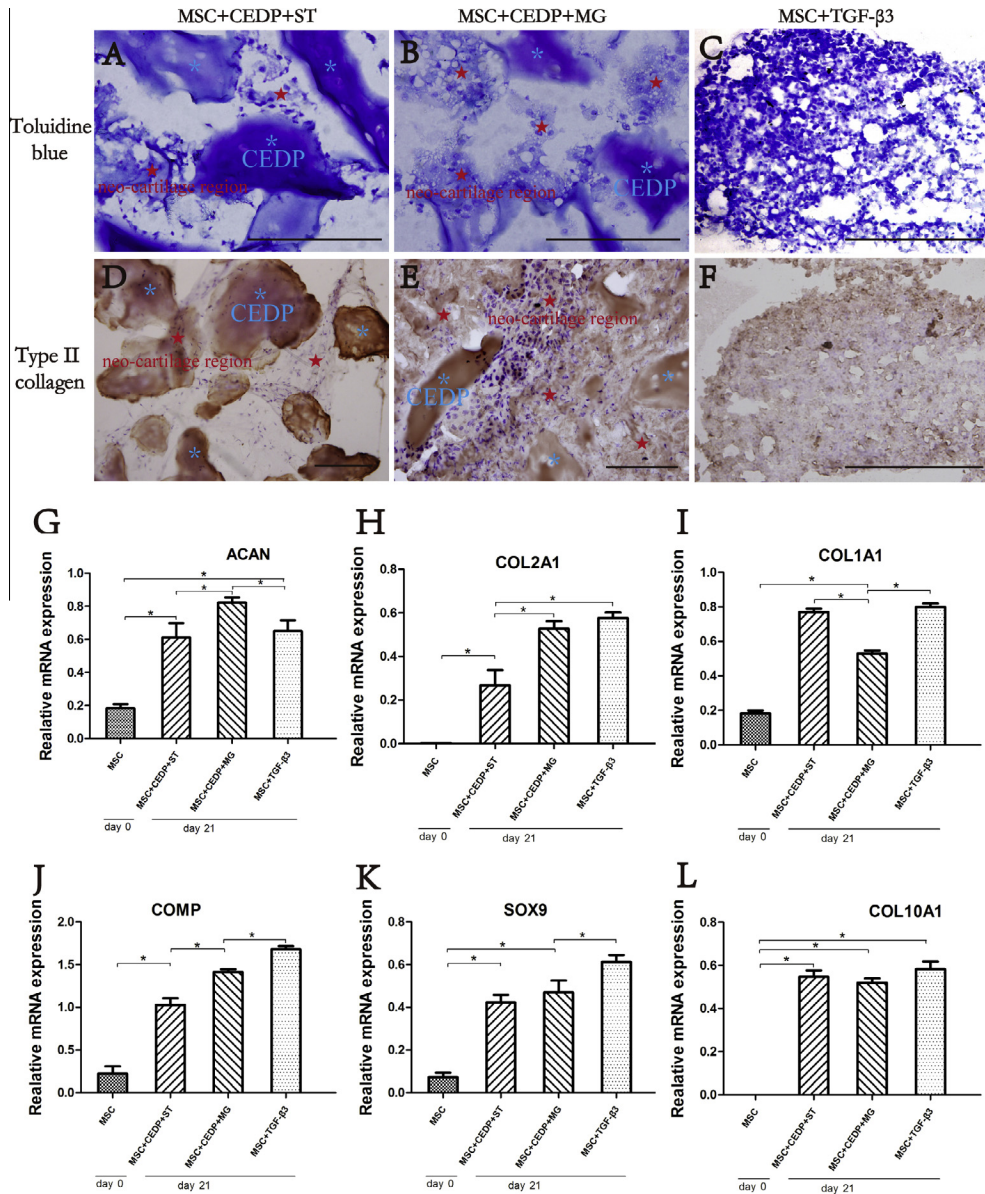
Fig. 7. Chondrogenic differentiation *in vitro*. Comparison of proteoglycan deposition using toluidine blue staining (A–C), type II collagen expression (D–F), and expression of chondrogenic markers (G–L) of representative aggregates obtained on day 21. MG indicates microgravity; ST indicates static; ★indicates neo-cartilage region; ✩indicates residual CEDP. The results are the means ± SD (n = 5), $^*p$ < 0.01. Scale bar: 200 μm in (A, B, D, E), 100 μm in (C, E).

regeneration. Before implantation, rat BMSCs were labeled with green fluorescent protein by infection with GFP lentivirus (Fig. 12A and E). Image tracking indicated that GFP-positive cells could be detected in the repaired areas of the experimental right knee at 2 and 12 weeks after surgery, whereas no GFP-positive cells were found in the left knee (Fig. 12B and F). In addition, cryosections of the repaired tissue confirmed that remaining CEDPs and GFP-BMSCs were found on the defect site in the early stage after implantation (2 weeks after surgery) (Fig. 12C and G). At 12 weeks, GFP-positive cells were also present in the repair tissue (Fig. 12D and H).

3.9. Micro-CT analysis

A certain amount of bone regeneration can be found in three groups, both at 6 and 12 weeks after surgery (Fig. 13A). However, the volume of regenerated bone was greater in the CEDP + MSC

group than in the two other groups. The ratio of bone to tissue volume (BVF) was significantly higher in the CEDP + MSC group than in the two other groups (p < 0.01), and the CEDP group was significantly higher than the Fibrin group (p < 0.01), both at 6 and 12 weeks. For each specific group, there was a significant difference between 6 and 12 weeks. Concerning the Tb.Th value, there was no significant difference among the three groups at 6 weeks (p > 0.05), while the CEDP + MSC group was higher than the Fibrin group at 12 weeks (p < 0.05). For each specific group, there was a significant difference between 6 and 12 weeks (Fig. 13B and C).

4. Discussion

Cartilage regeneration remains a difficult clinical issue due to the limited capacity for self-repair of cartilage as a result of its avascular structure [1,2,8]. Autologous chondrocyte implantation (ACI) is one of the most commonly used strategies for cartilage
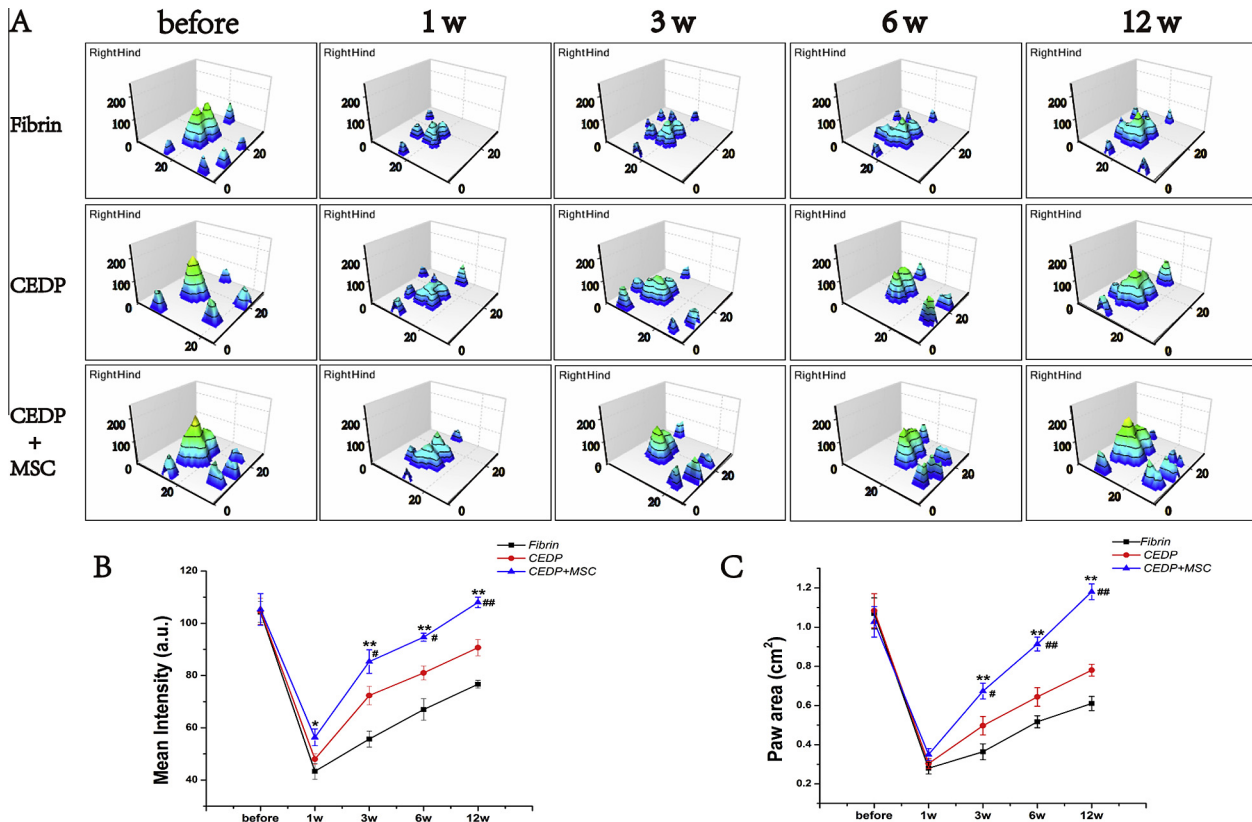
Fig. 8. Catwalk for gait analysis. (A) 3D footprint intensity images of the right hind leg in the various experimental groups at 1, 3, 6, and 12 weeks after surgery. Time course of the weight load measured as mean intensity (B) and the paw area (C). The results are the means ± SD ($n = 6$), $^{*}p < 0.05$, $^{**}p < 0.01$ compared to Fibrin group, and $\#p < 0.05$, $\#\#p < 0.01$ compared to the CEDP group.

repair and has been shown to have satisfactory therapeutic effects [33,34]. However, this method has a number of shortcomings, such as insufficient cell numbers, donor site morbidity, and chondrogenic phenotype loss along with monolayer chondrocyte cell expansion, which hamper its widespread adoption in clinical practice. Furthermore, two operations are required for this strategy – the first operation is performed to harvest chondrocytes from the patient, and after *in vitro* expansion, the chondrocytes are reimplanted in sufficient numbers into the same patient through a second surgery [35]. Considering these limitations, in the present study, we proposed a method to prepare a novel cell carrier derived from natural cartilage ECM, termed cartilage ECM-derived particles (CEDPs), which can support proliferation of MSCs and facilitate their chondrogenic differentiation. Further, the MSC-laden CEDPs microtissue aggregates can be used directly for cartilage repair *in vivo*. This strategy for cell culture, stem cell differentiation and the one-step surgery for cartilage repair provide novel prospects for cartilage tissue engineering and may have further broad clinical applications.

Previous studies indicated that microcarrier culture of MSCs promoted proliferation and differentiation [17,18]. The microcarrier composition determines its biocompatibility, and is also a crucial factor that affects the behavior of cells [19]. Hong et al. reported that microcarrier coated with ECM components had better biocompatibility and was conducive to cell adhesion [20]. Sutherland et al. reported that PLGA microspheres encapsulated with decellularized cartilage can induce chondrogenesis of rat marrow-derived MSCs without the use of exogenous growth factors [36]. We expected that microcarriers consisting of cartilage ECM would exhibit a strong ability to support cell adhesion and provide a microenvironment facilitating MSC chondrogenic

differentiation. In this study, fresh goat cartilage was physically pulverized into particles. Then, particles with a median diameter of 263 μm, similar in size to commercial microcarriers, were selected by passing through sieves with the corresponding pore size. Moreover, as cartilage is a compact tissue, shattering into particles facilitates solution penetration, thus improving the efficiency of further decellularization. To remove the immunogenicity caused by cellular constituents, complete decellularization is required. We investigated various methods for decellularization, and finally formulated a satisfactory protocol in which CEDPs were treated with 1% SDS to remove cells followed by nucleases (50 U/mL DNase and 1 U/mL RNase) to digest residual nuclear acid components. After decellularization, CEDPS were washed with sterile PBS repeatedly to remove the residual reagents. MTT assay revealed no toxicity in the CEDPs (data not shown). This protocol was shown to remove DNA to a great extent (97.24% DNA removal) and retain relatively high levels of GAG components (88.74% sGAG retained). With these processes, we successfully prepared decellularized cartilage ECM-derived particles (CEDPs) with a round, oval, or irregular shape. Unlike most microcarriers reported to date, CEDPs are rich in natural cartilage ECM, and did not require treatment with any potentially toxic crosslinking agents.

When BMSCs and CEDPs were co-cultured in RCCS or under static conditions, most cells adhered to the CEDPs within 24 h and were subsequently able to differentiate into chondrocytes without the use of exogenous growth factors, as indicated by the detection of proteoglycan deposition, type II collagen synthesis, and the upregulation of chondrogenic markers (ACAN, Col2A1, COMP, SOX9). The microenvironment is a vital factor that affects stem cell fate. CEDPs derived from cartilage ECM may provide a natural chondrogenic niche for stem cells to differentiate toward chondrocytes.
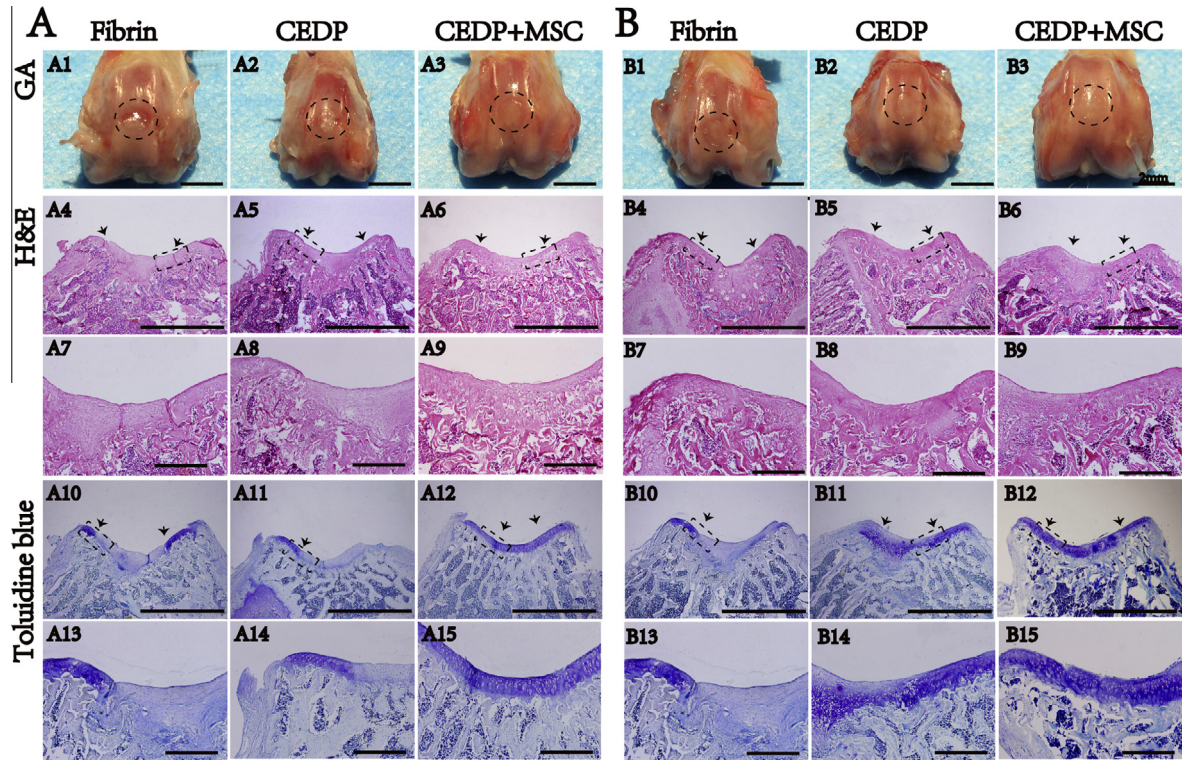
Fig. 9. Macroscopic observation and histological evaluation of repaired tissue at 6 and 12 weeks after surgery. Gross appearance of the repaired cartilage defects in the three groups (A1–A3, B1–B3). Dotted circles indicate cartilage defect areas in the three groups. Hematoxylin and eosin staining (A4–A9, B4–B9) and toluidine blue staining (A10–A15, B10–B15) of repaired knees. The black arrows indicate the edge of the defect, and the rectangle indicates the area shown in the under column at higher magnification. Scale bar: 2 mm in (A1–A6, A10–A12, B1–B6, B10–B12), 500 μm in (A7–A9, A13–A15, B7–B9, B13–B15). (For interpretation of the references to color in this figure legend, the reader is referred to the web version of this article.)
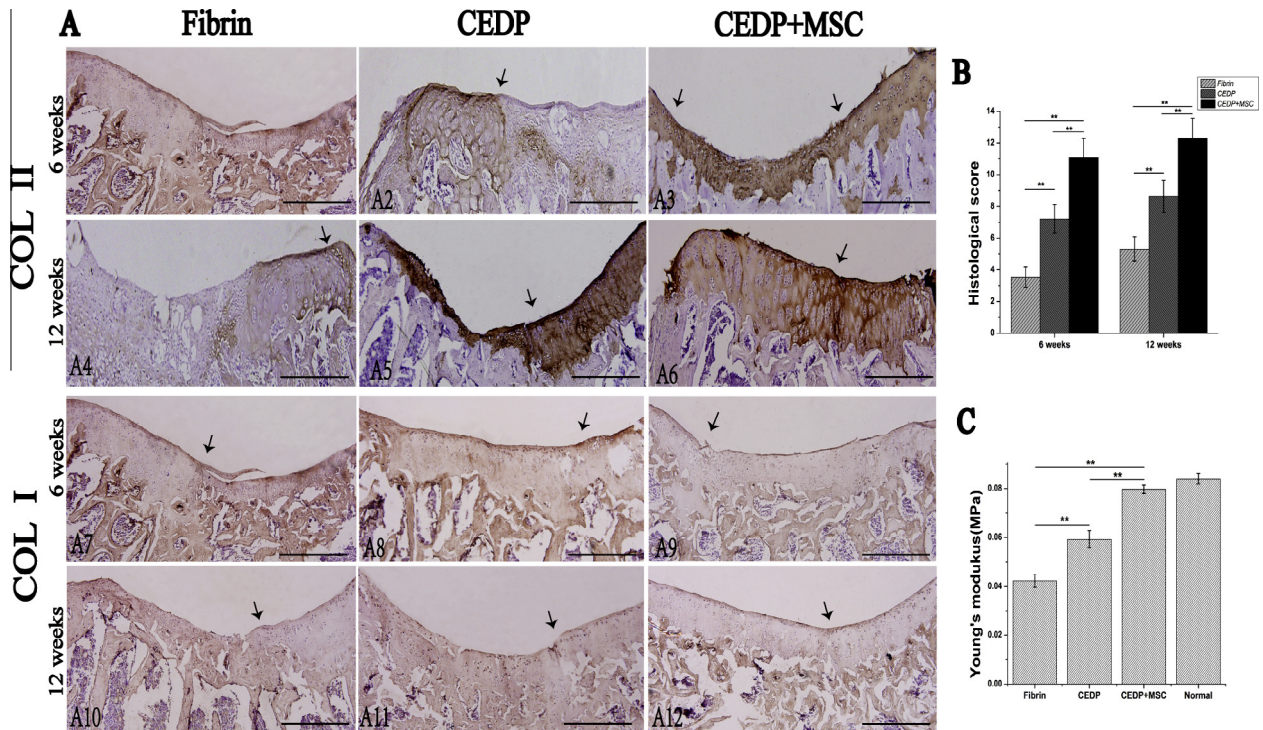
Fig. 10. Immunohistochemical staining and biomechanical evaluation. Immunohistological staining for type II collagen and type I collagen (A) at 6 and 12 weeks after surgery. (B) Histological scores of the repaired tissue at 6 and 12 weeks after surgery. (C) Young's modulus of the neo-cartilage at 12 weeks after surgery. The arrows indicate the edge of the defect. Scale bar: 500 μm.
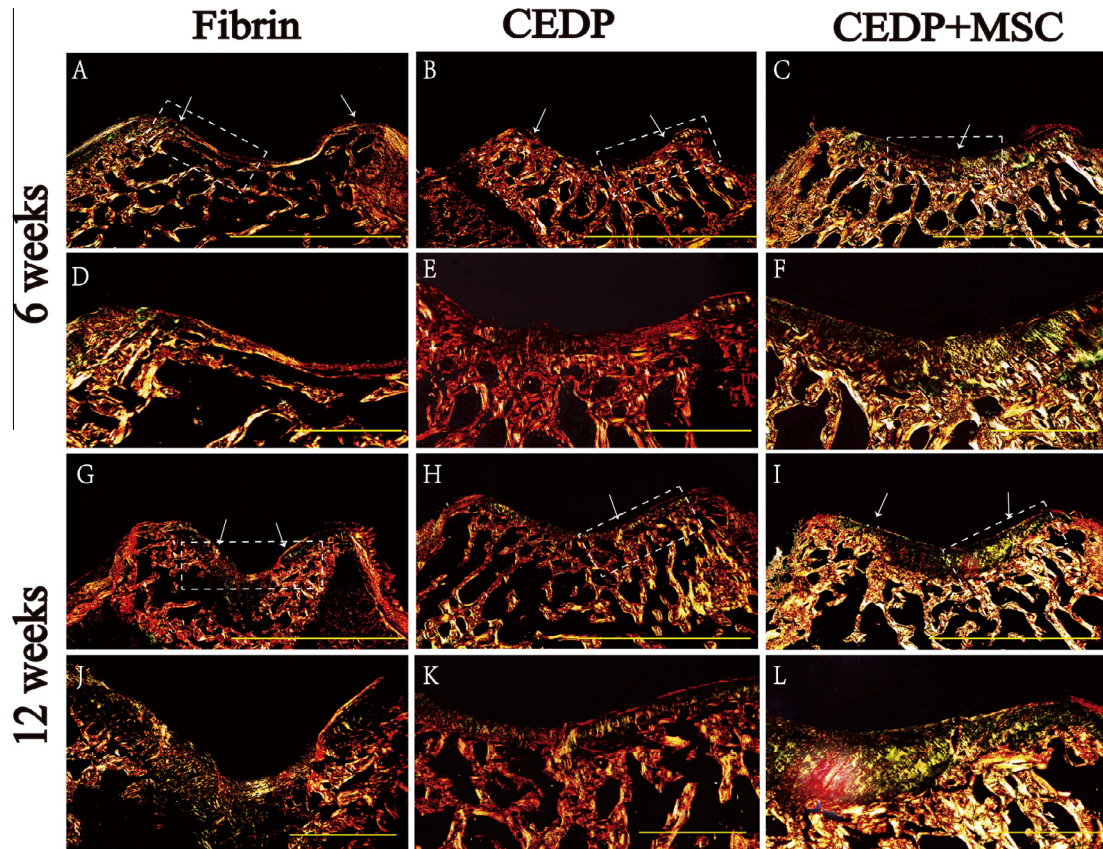
Fig. 11. Polarized microscopic findings by Sirius red staining of repaired tissue at 6 and 12 weeks after surgery. The black arrows indicate the edge of the defect, and the rectangle indicates the area shown in the under column at higher magnification. Scale bar: 2 mm in (A–C, G–I), 500 μm in (D–F, J–L). (For interpretation of the references to color in this figure legend, the reader is referred to the web version of this article.)
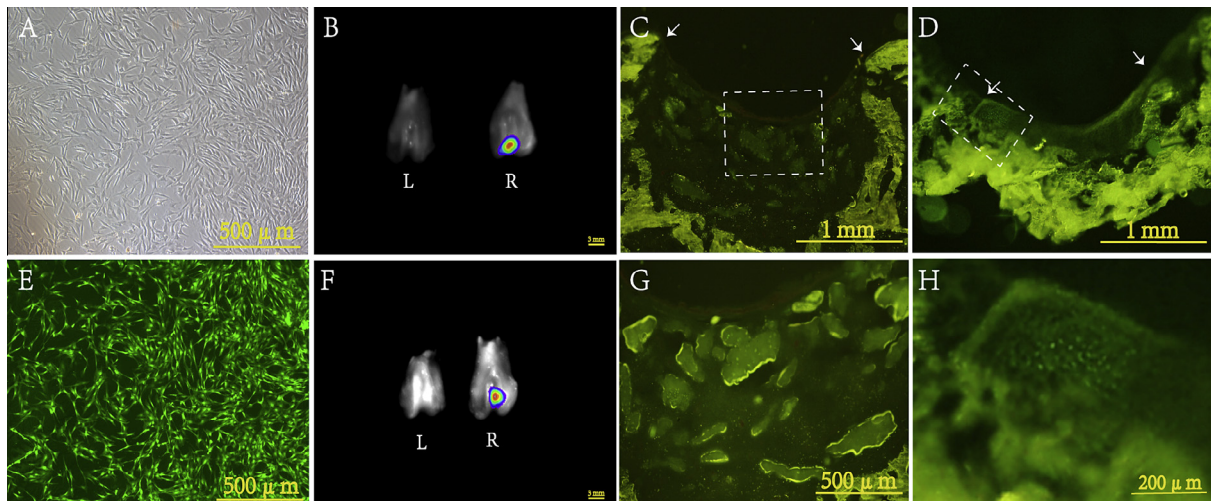

Fig. 12. GFP-positive cells tracking. Phase-contrast light micrograph (A) and fluorescence micrograph (E) of GFP-BMSCs. Visualization of GFP-positive cells by Kodak *In Vivo* Imaging Systems FX at 2 weeks (B) and 12 weeks (F) after surgery. "L" indicates left knee, "R" indicates right knee. Fluorescence microscopy images of cryosections from the repaired tissue at 2 weeks (C, G) and 12 weeks (D, H) after surgery.

In addition, certain bioactive factors or functional proteins remaining in CEDPs may play an important role in the chondrogenesis of MSCs [22–24]. Further studies are needed to explore the precise mechanism by which CEDPs influence stem cell fate.

The rotary cell culture system (RCCS) is a three-dimensional dynamic culture system that facilitates more efficient gas, liquid, oxygen, nutrient, and waste transfer [37]. The RCCS also provides a simulated microgravity environment to effectively induce chondrogenesis [38]. Our research also demonstrated that ACAN, COL2A1, and COMP gene expression levels were significantly higher in the MSC + CEDP + MG group than the MSC + CEDP + ST group, indicating that microgravity markedly enhanced the chondrogenesis of BMSCs in the MSC + CEDP + MG group. This result was consistent with the previous observations of Ohyabu and Bo,
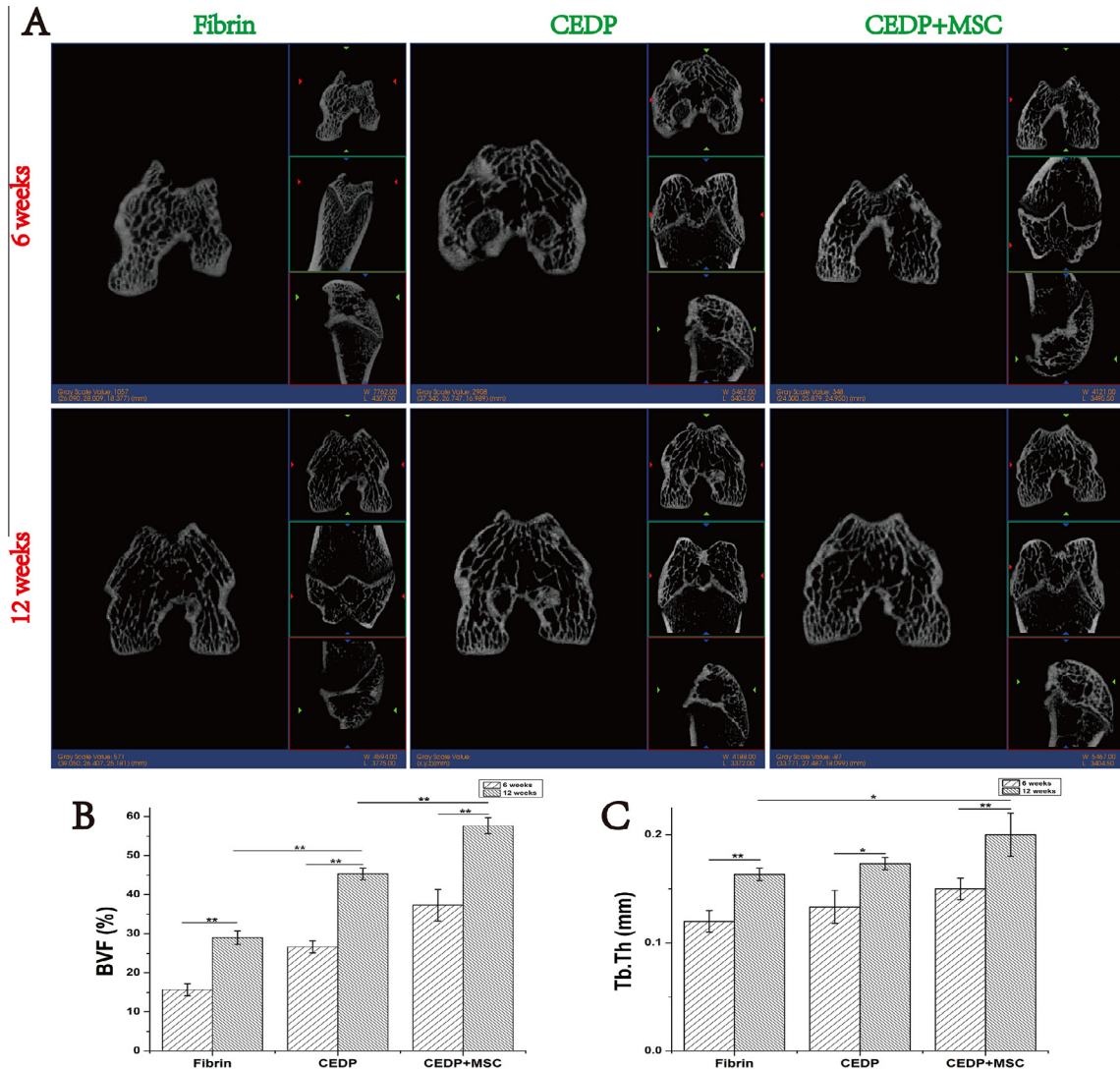
Fig. 13. Micro-CT imaging and analysis. (A) 2-D micro-CT images of repaired knee at 6 and 12 weeks after surgery. (B) The ratio of bone volume to tissue volume (BVF). (C) The thickness of trabecular bone (Tb.Th). The results are the means ± SD ($n = 6$), $^*p < 0.05$, $^{**}p < 0.01$.

who reported that the continuous mechanical stress caused by medium flow and microgravity associated with low shear facilitate the chondrogenesis of stem cell [38,39].

With extended culture time, large aggregations of cell-laden CEDPs developed into cartilage-like material, which we termed as functional cartilage microtissue. The functional cartilage microtissue is made up of MSC-laden CEDPs, which are connected by matrix secreted by cells on their surfaces. This may be an effective way to construct tissue engineered cartilage. The functional cartilage microtissue is rich in natural cartilage ECM, which is the basic material for cartilage regeneration and provides a natural cartilaginous microenvironment for cell differentiation and proliferation, thus promoting superior cartilage regeneration. Further, we explored the direct use of the functional cartilage microtissue as building blocks for cartilage repair *in vivo*. Native hyaline-like articular cartilage repair was found in the CEDP + MSC group as indicated by histological evaluations. Catwalk for gait analysis indicated that animals in the CEDP + MSC group showed rapid and good recovery of joint function. The repaired tissue in the CEDP + MSC group possessed similar mechanical properties to the native cartilage. The BVF value in the CEDP + MSC group was also higher than in the other two groups. In conclusion, cartilage

microtissue can lead to superior articular cartilage repair in a rat model. In addition, GFP-labeled cell tracking demonstrated that the implanted GFP-BMSCs can survive in the cartilage defect sites at both 2 and 12 weeks after surgery and contributed to neocartilage formation.

Despite considerable advances in cartilage tissue engineering, means of constructing large cartilage tissue for larger-scale cartilage defect repair remain to be developed. This study may provide insights to overcome this challenging issue. In clinical practice, BMSCs can be harvested from the patient before the operation, and then co-cultured with CEDPs in a bioreactor to facilitate chondrogenesis of BMSCs and to form tissue engineered cartilage microtissue. The size of the microtissue can be controlled by regulating mixing intensity and duration of culture to best fit the characteristics of the desired cartilage defect. In addition, MSC-seeded CEDP microtissue aggregates can also be delivered arthroscopically into the cartilage defect sites, which would reduce surgical trauma. There are two possible sources of decellularized cartilage ECM for CEDP preparation. The first source of decellularized cartilage ECM is from deceased human donors. Biocartilage (Arthrex) which is dehydrated, micronized allogeneic cartilage has been used in clinical treatment [40]. However, there is a critical shortage of such

donors. The other source is from xenogeneic decellularized cartilage ECM. According to the reports, several commercialized decellularized scaffolds, including dermis tissue (Alloderm®; LifeCell), porcine heart valves (Synergraft®; Cryolife) and porcine urinary bladder (Urinary bladder matrix; ACell) have received FDA approval for use in humans.

This strategy is also applicable for other types of tissue or organ injury in which it is necessary to repair large defects. Blokhuis et al. demonstrated a similar approach in bone tissue engineering, in their study, cell-seeded calcium phosphate particles were used to fill ovine segmental defects [41]. Thus, for large tissue engineered tissue or organ fabrication, it may be possible to first construct bioactive and functional "tissue engineered microtissue" using particles derived from the ECM of the desired tissue or organ. Then, tissue engineered microtissues can be gathered to build large tissues or artificial organs.

5. Conclusion

In this study, we proposed a method for preparing a novel cell carrier derived from natural cartilage ECM, termed cartilage ECM-derived particles (CEDPs), and further functional cartilage microtissue formation for cartilage repair. The results of an *in vitro* study indicated that CEDPs could support MSC attachment, proliferation, and facilitate their chondrogenic differentiation without the use of exogenous growth factors. Further, the direct use functional cartilage microtissue induced hyaline-like articular cartilage repair *in vivo*. This strategy for cell culture, stem cell differentiation, and the one-step surgery using cartilage microtissue for cartilage repair provides a new approach for cartilage regeneration and repair. In addition, this approach may provide novel prospects for the tissue engineering of a wide variety of tissues.

Disclosure

The authors have no conflict of interest to disclose.

Acknowledgments

References

[1] E.B. Hunziker, Articular cartilage repair: are the intrinsic biological constraints undermining this process insuperable?, Osteoarthritis Cartilage 7 (1999) 15–28

[2] B. Johnstone, M. Alini, M. Cucchiarini, G.R. Dodge, D. Eglin, F. Guilak, et al., Tissue engineering for articular cartilage repair the state of the art, Eur. Cells Mater. 25 (2013) 248–267.

[3] R.N. Shah, N.A. Shah, M.M. Del Rosario Lim, C. Hsieh, G. Nuber, S.I. Stupp, Supramolecular design of self-assembling nanofibers for cartilage regeneration, Proc. Natl. Acad. Sci. USA 107 (2010) 3293–3298.

[4] C. Gaut, K. Sugaya, Critical review on the physical and mechanical factors involved in tissue engineering of cartilage, Regener. Med. 22 (2015) 1–15.

[5] R.L. Dahlin, L.A. Kinard, J. Lam, C.J. Needham, S. Lu, F.K. Kasper, A.G. Mikos, Articular chondrocytes and mesenchymal stem cells seeded on biodegradable scaffolds for the repair of cartilage in a rat osteochondral defect model, Biomaterials 35 (2014) 7460–7469.

[6] G.A. Matricali, G.P.E. Dereymaeker, F.P. Luyten, Donor site morbidity after articular cartilage repair procedures: a review, Acta Orthopaedica Belgica 76 (2010) 669–674.

[7] E.M. Darling, K.A. Athanasiou, Rapid phenotypic changes in passaged articular chondrocyte subpopulations, J. Orthopaedic Res. 23 (2005) 425–432.

[8] N. Georgi, C. van Blitterswijk, M. Karperien, Mesenchymal stromal/stem cell-or chondrocyte-seeded microcarriers as building blocks for cartilage tissue engineering, Tissue Eng. Part A 20 (2014) 2513–2523.

[9] L. Song, D. Baksh, R.S. Tuan, Mesenchymal stem cell-based cartilage tissue engineering: cells, scaffold and biology, Cytotherapy 6 (2004) 596–601.

[10] Q. Yang, J. Peng, Q. Guo, J. Huang, et al., A cartilage ECM-derived 3-D porous acellular matrix scaffold for in vivo cartilage tissue engineering with PKH26-labeled chondrogenic bone marrow-derived mesenchymal stem cells, Biomaterials 29 (2008) 2378–2387.

[11] H. Kang, J. Peng, S. Lu, et al., In vivo cartilage repair using adipose-derived stem cell-loaded decellularized cartilage ECM scaffolds, J. Tissue Eng. Regener. Med. 8 (2014) 442–453.

[12] Y.Y. Li, H.W. Cheng, K.M. Cheung, D. Chan, B.P. Chan, Mesenchymal stem cell-collagen microspheres for articular cartilage repair: cell density and differentiation status, Acta Biomater. 10 (2014) 1919–1929.

[13] L.E. Freed, G. Vunjak-Novakovic, R. Langer, Cultivation of cell-polymer cartilage implants in bioreactors, J. Cell. Biochem. 51 (1993) 257–264.

[14] J. Malda, C.A. van Blitterswijk, M. Grojec, D.E. Martens, J. Tramper, J. Riesle, Expansion of bovine chondrocytes on microcarriers enhances redifferentiation, Tissue Eng. 9 (2003) 939–948.

[15] K. Schrobback, T.J. Klein, R. Crawford, Z. Upton, J. Malda, D.I. Leavesley, Effects of oxygen and culture system on in vitro propagation and redifferentiation of osteoarthritic human articular chondrocytes, Cell Tissue Res. 347 (2012) 649–663.

[16] K. Schrobback, T.J. Klein, M. Schuetz, Z. Upton, D.I. Lea-vesley, J. Malda, Adult human articular chon-drocytes in a microcarrier-based culture system: expansion and redifferentiation, J. Orthopaedic Res. 29 (2011) 539–546.

[17] D. Schop, F.W. Janssen, E. Borgart, J.D. de Bruijn, R. van Dijkhuizen-Radersma, Expansion of mesenchymal stem cells using a microcarrier-based cultivation system: growth and metabolism, J. Tissue Eng. Regener. Med. 2 (2008) 126–135.

[18] M. Mathieu, S. Vigier, M.N. Labour, C. Jorgensen, E. Belamie, D. Noël, Induction of mesenchymal stem cell differentiation and cartilage formation by cross-linker-free collagen microspheres, Eur. Cell Mater. 28 (2014) 82–96.

[19] J. Malda, C.G. Frondoza, Microcarriers in the engineering of cartilage and bone, Trends Biotechnol. 24 (2006) 299–304.

[20] Y. Hong, C. Gao, Y. Xie, Y. Gong, J. Shen, Collagen-coated polylactide microspheres as chondrocyte microcarriers, Biomaterials 26 (2005) 6305–6313.

[21] D. Philp, S.S. Chen, W. Fitzgerald, J. Orenstein, L. Margolis, H.K. Kleinman, Complex extracellular matrices promote tissue-specific stem cell differentiation, Stem Cells 23 (2005) 288–296.

[22] C.C. Chen, C.H. Liao, Y.H. Wang, Y.M. Hsu, S.H. Huang, C.H. Chang, H.W. Fang, Cartilage fragments from osteoarthritic knee promote chondrogenesis of mesenchymal stem cells without exogenous growth factor induction, J. Orthopaedic Res. 30 (2012) 393–400.

[23] N.C. Cheng, B.T. Estes, H.A. Awad, F. Guilak, Chondrogenic differentiation of adipose-derived adult stem cells by a porous scaffold derived from native articular cartilage extracellular matrix, Tissue Eng. Part A 15 (2009) 231–241.

[24] A.J. Sutherland, E.C. Beck, S.C. Dennis, G.L. Converse, R.A. Hopkins, C.J. Berkland, M.S. Detamore, Decellularized cartilage may be a chondroinductive material for osteochondral tissue engineering, PLoS ONE 10 (2015) e0121966.

[25] F.H. Albrecht, Closure of joint cartilage defects using cartilage fragments and fibrin glue, Fortschr. Med. 101 (1983) 1650–1652.

[26] Y. Lu, S. Dhanaraj, Z. Wang, D.M. Bradley, S.M. Bowman, B.J. Cole, F. Binette, Minced cartilage without cell culture serves as an effective intraoperative cell source for cartilage repair, J. Orthopaedic Res. 24 (2006) 1261–1270.

[27] N. Wang, S. Grad, M.J. Stoddart, P. Niemeyer, K. Reising, H. Schmal, N.P. Südkamp, M. Alini, G.M. Salzmann, Particulate cartilage under bioreactor-induced compression and shear, Int. Orthop. 38 (2014) 1105–1111.

[28] C. Maniatopoulos, J. Sodek, A.H. Melcher, Bone formation in vitro by stromal cells obtained from bone marrow of young adult rats, Cell Tissue Res. 254 (1988) 317–330.

[29] F.P. Hamers, A.J. Lankhorst, T.J. van Laar, W.B. Veldhuis, W.H. Gispen, Automated quantitative gait analysis during overground locomotion in the rat: its application to spinal cord contusion and transection injuries, J. Neurotrauma 18 (2001) 187–201.

[30] S. Zhang, Y.Z. Jiang, W. Zhang, L. Chen, T. Tong, W. Liu, Q. Mu, H. Liu, J. Ji, H.W. Ouyang, X. Zou, Neonatal desensitization supports long-term survival and functional integration of human embryonic stem cell-derived mesenchymal stem cells in rat joint cartilage without immunosuppression, Stem Cells Dev. 22 (2013) 90–101.

[31] S. Wakitani, T. Goto, S.J. Pineda, et al., Mesenchymal cell-based repair of large, full-thickness defects of articular cartilage, J. Bone Joint Surg. Am. 76 (1994) 579–592.

[32] X. Shao, J.C. Goh, D.W. Hutmacher, E.H. Lee, G. Zigang, Repair of large articular osteochondral defects using hybrid scaffolds and bone marrow-derived mesenchymal stem cells in a rabbit model, Tissue Eng. 12 (2006) 1539–1551.

[33] L. Peterson, H.S. Vasiliadis, M. Brittberg, A. Lindahl, Autologous chondrocyte implantation: a long-term follow-up, Am. J. Sports Med. 38 (2010) 1117–1124.

[34] A.E. Beris, M.G. Lykissas, I. Kostas-Agnantis, G.N. Manoudis, Treatment of full-thickness chondral defects of the knee with autologous chondrocyte implantation: a functional evaluation with long-term followup, Am. J. Sports Med. 40 (2012) 562–567.

[35] L. Dai, Z. He, X. Zhang, X. Hu, L. Yuan, M. Qiang, J. Zhu, Z. Shao, C. Zhou, Y. Ao, One-step repair for cartilage defects in a rabbit model: a technique combining

the perforated decalcified cortical-cancellous bone matrix scaffold with microfracture, Am. J. Sports Med. 42 (2014) 583–591.

[36] A. Sutherland, M. Detamore, Bioactive microsphere-based scaffolds containing decellularized cartilage, Macromol. Biosci. 15 (2015) 979–989.

[37] L.J. Cummings, S.L. Waters, Tissue growth in a rotating bioreactor. Part II: fluid flow and nutrient transport problems, Math. Med. Biol. 24 (2007) 169–208.

[38] H. Gao, P.S. Ayyaswamy, P. Ducheyne, Dynamics of a microcarrier particle in the simulated microgravity environment of a rotating-wall vessel, Microgravity Sci. Technol. 10 (1997) 154–165.

[39] Y. Ohyabu, N. Kida, H. Kojima, T. Taguchi, J. Tanaka, T. Uemura, Cartilaginous tissue formation from bone marrow cells using rotating wall vessel (RWV) bioreactor, Biotechnol. Bioeng. 95 (2006) 1003–1008.

[40] A.M. Hirahara, K.W. Mueller Jr., BioCartilage: a new biomaterial to treat chondral lesions, Sports Med. Arthrosc. 23 (2015) 143–148.

[41] T.J. Blokhuis, B.W. Wippermann, F.C. den Boer, A. van Lingen, P. Patka, F.C. Bakker, H.J. Haarman, Resorbable calcium phosphate particles as a carrier material for bone marrow in an ovine segmental defect, J. Biomed. Mater. Res. 51 (2000) 369–375.